Nat. Hazards Earth Syst. Sci. Discuss., 1, 4063–4086, 2013
www.nat-hazards-earth-syst-sci-discuss.net/1/4063/2013/
doi:10.5194/nhessd-1-4063-2013

Natural Hazards and Earth System Sciences Discussions
Open Access

A new-type flexible rock-shed under the impact of rock block: experimental investigation

S. Shi[1], M. Wang[1], X. Peng[2], and Y. Yang[3]

[1]Department of Civil Engineering, Logistical Engineering University, Chongqing 401311, China
[2]School of Materials Science and Engineering, Shanghai Jiao Tong University, Shanghai 20030, China
[3]Geobrugg (Chengdu) Co., Ltd., Chengdu 611731, China

Received: 19 June 2013 – Accepted: 21 July 2013 – Published: 9 August 2013

Correspondence to: M. Wang (wangmin198217@163.com)

Published by Copernicus Publications on behalf of the European Geosciences Union.

Abstract

The main disadvantage of conventional concrete rock-shed is the need for a massive foundation due to the deadweight of the structure. In order to overcome such construction difficulty and to reduce costs, a new concept of flexible rock-shed is proposed in this paper. The flexible rock-shed is made of flexible nets held up by specially designed steel vaulted structure. An 1 : 1 prototype is manufactured and tested for functional evaluation with impact experiment. It is shown that the structure can stand for an impact energy of about 250 kJ without observable rupture of the flexible nets or cables and can be put into service again with some maintenances on the steel vaulted structure. Expermental data such as local strains, peak loads and impact times are recorded by dynamic strain gauges, load cells and high speed camera for structural analysis and some complementary suggestions of improving and designing are offered with respect to the joints and components.

1 Introduction

In mountain areas, rockfall always occurs randomly and suddenly. Special geological features and climate factors are the principal causal mechanisms (Sasiharan et al., 2006; Castro-Fresno et al., 2008; Volkwein et al., 2011). Rockfall can cause a lot of damage to highways, railways and infrastructure built along steep slopes and seriously restricts economy activities and transportation construction. The protection measures against rockfall consist of active methods and passive methods (Bertolo et al., 2009). The former methods, which include structures such as rock bolts, grouted bars, continuous concrete wall and anchored cable nets, are to prevent the detachment of blocks from their original position or to restrict the trajectory of the rockfall. The latter methods do not directly interfere in the process of rockfall, but control the dynamic effects of moving blocks. Embankments, ditches, passive barriers, and rock-sheds can be classified into passive methods.

NHESSD
1, 4063–4086, 2013

The active methods are often applied to cover or reinforce hazardous regions. However, in some cases, the regions are larger and these solutions are very costly and not effective. The passive methods, on the other hand, firstly involve the evaluation of possible paths of detachable rockfall and rockfall kinetic energy. Then the location is chosen for constructing the systems to prevent rockfall (Azzoni and de Freitas, 1995; Chau et al., 2002; Guzzetti et al., 2002; Giani et al., 2004; Topal et al., 2007). However, the trajectory of rockfall is difficult to predict due to the inherent randomness of rockfall. This makes these passive methods far from sufficient. To solve this problem, rock-shed was invented to directly cover the roads and other spots (Fig. 1). This structure is composed with reinforced concrete columns and foundation and a roof slab and has good stiffness and protection performance, but needs a massive foundation due to the deadweight of the structure. In addition, constructing such foundations along steep slopes with frequently poor quality bedrock is usually very difficult and expensive (Kirsten, 1982; Labiouse et al., 1996).

Over the past decades many research efforts have been devoted to overcome the disadvantages of rock-sheds by converting rigid rock-sheds into semi-rigid ones and achieving to reduce the impact load by rockfall, the weight of the structure, construction costs and difficulty. The widely used forms at this stage are covering a soil layer on the roof slab (Kishi et al., 2002; Pichler et al., 2005; Kawahara and Muro, 2006; Bhatti and Kishi, 2010), or developing a new rock-shed (Structurally Dissipating Rock-shed, SDR) made of reinforced concrete slabs held up by specially designed supports that act as a type of expendable fuse to absorb rockfall energy (Mougin et al., 2005; Delhomme et al., 2005, 2007). With the aim of developing a structure which is simple to build and adaptive to the requirements of emergency maintenance and construction, a new concept of flexible rock-shed is proposed in this paper, which can be manufactured at factory, field-assembled and especially suitable for convenient construction and emergency maintenance. The flexible rock-shed (Fig. 2) mainly composes of a steel vaulted structure and flexible nets. On the one hand this structure fully takes advantage of the flexibility, high strength and high impact resistance of flexible nets which can be designed with different assembly to meet different needs of impact resistance. On the other hand, easy processing and molding characteristics of metal materials are utilized for the steel vaulted structure to satisfy various structural forms with aesthetic advantages.

2 Design strategy of flexible rock-shed

The design strategy of the flexible rock-shed from concept to actual product is divided into three stages:

(1) design the configuration dimensions of the system based on the requirements of the protected subject, such as the width of the pass road, the limited height of the vehicles;

(2) according to energy range of rockfall investigated before, select the appropriate flexible nets and then design the support system, including the cross sectional sizes of the structural elements and the connection joints between the elements;

(3) calculate the force transferred from the structure and design the foundations of the flexible rock-shed.

The flexible rock-shed relies on the deformation of the flexible nets for energy absorption. In general case, the flexible nets can absorb more energy through larger deformation, but in design, adequate safety distance between the system and the ground to be protected must be taken into account. In accordance with the dimension requirements of two-way traffic line, the designed flexible rock-shed is a structure with 8.5 m in width, 5 m in span and 7.0 m in height (Fig. 3). There are longitudinal supports between two steel vaulted structures. In addition, compared to other reinforced concrete rock-sheds, the flexible rock-shed is designed to stand for an impact energy to about 250 kJ considering economical factors, safety distance and kinetic energy level of rockfall happened in normal conditions. If a higher demand for energy level is needed, multiple layers of flexible rock-sheds could be set up.

The speed of rockfall ranges from a few meters per second to up to 25 ∼ 30 $\mathrm{m\,s^{-1}}$ (Peila and Ronco, 2009) and owing to the fact that damages were frequently caused by impacts of small blocks with high velocities, producing the nets perforation, thus the maximum speed of rockfall impacted to the system is constrained to 25 $\mathrm{m\,s^{-1}}$ (Cazzani et al., 2002; Volkwein et al., 2011; Spadari et al., 2012). An 1 : 1 prototype of flexible rock-shed (Fig. 4a) with a vaulted structure is designed and manufactured (Fig. 4b), in which flexible nets are chosen to be subjected to direct impact. The flexible nets are composed of ring nets and TECCO wire meshes G65 (Fig. 4c). The kinetic energy from rockfall is dissipated directly by the elastic-plastic deformation of the flexible nets, cables and the steel vaulted structure in case of a central impact. For impacts on the edges, the system can absorb energy of rockfall without structural damage.

3 Experimental analysis of rock block impact on flexible rock-shed

Passive barriers consist of flexible nets supported by steel cables with inelastic brake elements and columns and have been constructed worldwide, resulting in the development of different national testing procedures (Gerber, 2001; EOTA, 2008). The current flexible rock-shed is a combination of passive barriers and rock-shed. Accordingly, the procedure for testing the flexible rock-shed is designed with reference to testing procedures of passive barrier and reinforced concrete rock-shed. Prefabricated 14-face polyhedron reinforced-concrete block is used to simulate rockfall (Fig. 5a). In the experiment, the mass of the reinforced-concrete block is approximately 800 kg, and the density is $\rho = 2500\,\mathrm{kg\,m^{-3}}$. A steel cable hanger (Fig. 5a) with a volume of $V_1 = 769.23\,\mathrm{cm^3}$ is embedded beforehand for hoisting the block by a crane. The edge

NHESSD
1, 4063–4086, 2013

length b of the block can be calculated as:

$$b = \left[\left(\frac{m}{\rho} + V_1\right) \times \frac{81}{77}\right]^{\frac{1}{3}}. \quad (1)$$

The tests involve dropping the block from a given height in order to obtain a fixed energy of 250 kJ and an impacting velocity of 25 m s^{-1}. The height lifted by the crane and the impact velocity are calculated by the formula below:

$$h = \frac{E}{mg} + h_1, \quad v = \sqrt{2g(h - h_1)} \quad (2)$$

where E is the kinetic energy of the block; h_1 is the height of the flexible rock-shed; g is the acceleration of gravity.

The block is lifted to the dropping height about 39 m. To ensure that the block can be released freely, an unhooking apparatus is designed and installed between the hanger and the block (Fig. 5b). The unhooking apparatus can be remotely manipulated to implement free fall of the block. A plumb line is used to determine the impacting position so that the block can fall along with the plumb line and impact on the mid-span of the system, as shown in Fig. 3b. This makes the response of the steel vaulted structure under impact be symmetrical. Dynamical strain gauges are pasted on half of the steel vaulted structure and connected to a data acquisition station. The pasted strain gauges are located at T0, T1-1, T1-2, T1-3, T1-4 and T1-5, as shown in Fig. 3a. There are strain gauges along three directions at T0, T1-1, and T1-2, and one direction is along with the hoop of the flexible rock-shed, the other is along with the axis of the rock-shed and the last is 45° with the axis of the rock-shed. There are strain gauges along two directions at T1-3, T1-4, and T1-5, and one direction is along with the hoop of the flexible rock-shed, the other is along with the axis of the rock-shed. A high-speed camera (300 frames s^{-1}) is used to record the impact of the block onto the system. Load cells are used for the measurement of tensile force acting on the cable anchors and the horizontal cables (Fig. 3a). Experimental data is stored for subsequent extraction.

NHESSD
1, 4063–4086, 2013

4 Experimental results and discussions

From the high-speed camera recorded frames, the time elapse T between the first contact of the block with the flexible rock-shed and a concerned time can be evaluated by:

$$T = \frac{f_2 - f_1}{f} \tag{3}$$

where f_1 is the number of frames at the first time of the block contacted the rock-shed; f_2 is the number of frames corresponding to the concerned time; f is the recording frequency.

Key point frames of video camera as recorded during the impact phase are selected (Fig. 6), including that the block contacting with rock-shed (the 15th frame), the block down to the lowest point and the steel vaulted structure beginning to rebound (the 58th frame), the block still rebounding and the steel vaulted structure stopping rebounding (the 83th frame), the block rebounding off flexible rock-shed (the 175th frame) and the block flying off one side of the rock-shed (the 500th frame). The respective time elapses can be calculated from Eq. (3) and are listed in Table 1. In addition, the maximum deformation of the flexible nets is also clearly visible in Fig. 6 and the maximum loads acting on the cable anchor and horizontal cable are recorded by the load cells and are listed in Table 2.

As can be seen in Fig. 6, the flexible rock-shed successfully withstands the impact of the block with a kinetic energy of about 250 kJ and no rupture of the flexible nets and cables is observed. In the impacting process, when the block rebounds, the steel vaulted structure rebounds simultaneously, but part of residual deformation is preserved. At this moment, some components of the rock-shed absorb a large portion of impact energy through elastic-plastic deformation. The steel vaulted structure undergoes plastic distortion but can continue to be used after some maintenance. As shown in Table 1, the impacting time period is 0.143 s followed by a rebounding period up to 1.617 s. As can be seen in Table 2, the maximum deformation of the flexible nets is 2.31 m, resulting in a safety distance of 4.690 m which is greater than traffic vehicle height (maximum 4.0 m). The loads on the cable anchor and horizontal cable are 21.4 kN and 29.5 kN, respectively. So the construction of the cable anchor used in the system is easier and the diameter of the horizontal cable can be reduced compared to the current design with diameter 18 mm (the tensile load is greater than 190 kN) or even can be canceled.

Figure 7 shows the strain history at various locations as recorded by the strain gauges. It represents a typical time-history of strains throughout a free fall impact test, and in Fig. 7a, strains on the steel vaulted structure at each pasting location first rapidly increase and reach the peak in a time interval of about 0.14 s, then the block and steel vaulted structure are rebounding until the structure stopping rebounding, strains decrease and reach the stability in a time interval of about 0.25 s. The results coincide well with data obtained by the high-speed camera. At the pasting locations T0, T1-1 and T1-2, residual strains are observed after stabling, indicating permanent plastic deformation renders within the range of the pasting locations. However, at the pasting locations T1-3, T1-4 and T1-5, the strains stabilizes at approximately 0. Therefore, at these three pasting locations, the deformation is nearly elastic which indicates that the load on the column of the steel vaulted structure is small, and the cross section sizes of the columns and shearing supports can be decreased compared to the current design. The design of the flexible rock-shed does not need a massive foundation due to the flexibility of the structure and construction of such foundations is easier and cheaper than the reinforced concrete rock-shed. Figure 7 also shows that the peak values of strain at T0 and T1-1 and the values of residual strains after stabilizing are higher by nearly one order of magnitude than those at other measuring locations. Thus, more serious distortion of the steel vaulted structure occurs within the range of T0 and T1-1.

Under the impact of the block, longitudinal support cables and flexible nets together cause the inward inclination of the net-hanging bracket and the angle is about 35°, resulting in the distortion of the arched beams (Fig. 8a). The Longitudinal supports at the two sides of mid-span support the steel vaulted structure, and therefore the

NHESSD
1, 4063–4086, 2013

most serious distortion occurs between the two longitudinal supports nearly mid-span (Fig. 8b).

An 1-1 cross section near the two longitudinal supports at mid-span is selected and the detail deformation is shown in Fig. 8c. The solid lines indicate the non-distorted cross section of arched beam, while the dashed lines indicate the distorted cross section of arched beam (without considering the distortion of the cross section of the arched beam). As can be seen in Fig. 8c, due to the effect of stiffened plates connected to the net-hanging bracket between the top and the bottom flanges of the arched beam, the top and the bottom flange plates rotated inside simultaneously. Stiffened plates on one side were subjected to compression force and on the other side were subjected to tensile force. Because the external load is greater than the restriction effect of the stiffened plates and the bending capacity differed between stiffened plates and the top and the bottom flanges of the arched beam, serious distortion occurred at the arched beam and the stiffened plates. As a result, the capability of stiffened plates to restrict general distortion was deduced, and the flanges and web plant of the arched beams were distorted. In order to increase the capacity of the stiffened plants to restrict the distortion of the structure, the width and the thickness of the stiffened plants should be increased.

The forces applied on the gusset plates welded to the top flanges, bottom flanges of the arched beam and the longitudinal supports are complicated, including shearing forces, bending moments and axial forces, the local welding is easier to be broken off. As can be seen in Figs. 6d and 9a, one of the gusset plates is failed and the local welding spot is broken off, and the other gusset plates buckled and the flanges deflected seriously (Fig. 9b). The longitudinal supports did not deform much because the welding locations between the gusset plates and the top and bottom flanges were too weak and could be easily damaged. Therefore, in order to restrict the distortion of the arch beams, the longitudinal supports should be directly connected to web plate of the beam and the thickness at connection location between longitudinal support and web plate of the beam should be increased to prevent local damage.

NHESSD
1, 4063–4086, 2013

Figure 10 shows the detail deformation of the components in the flexible rock-shed after the impact of the rock block. As can been seen in Fig. 10a, the ring nets and the wire meshes are all connected with the hoop cables by sewing cables. In the experiment, the sawing cables render no fracture and looseness. In addition, the cable clips are fixed and no sliding observed. The flexible nets are hanged down about 0.6 m because of the residual deformation after impact of the block. The longitudinal support cable directly impacted by the block is deformed much and the impact location of the cable retained at approximately 0.6 m bending trace. As can be seen in Fig. 10b, single rings in the ring nets do not deform much, and the ring nets on the whole do not undergo significant deformation and damage.

5 Conclusions

A new concept of flexible rock-shed protection structure is proposed and tested in this paper. The flexible rock-shed is mainly composed of a steel vaulted structure and flexible nets and can be manufactured at factory, field-assembled and especially suitable for convenient construction and emergency maintenance. Impact test is carried out to evaluate the functional performance of the flexible rock-shed. Testing results show that the rock-shed performs well under an impact of a rock block with 250 kJ energy and velocity of 25 $\mathrm{m\,s^{-1}}$. Due to the flexibility of the structure, the loads on the column, cable anchor and the horizontal cable are smaller and the section of the column and shearing support and the diameter of the horizontal cable can be reduced. In addition, in order to minimize the possibility of steel vaulted structure damage and to decrease the maintenance costs on the structure, the width and the thickness of the stiffened plants should be increased and the longitudinal supports should be directly connected to web plate of the beam and the thickness at connection location between longitudinal support and web plate of the beam should be increased to prevent local damage.

NHESSD
1, 4063–4086, 2013

Acknowledgements. The present research is funded by the National Science and Technology Support Program (2012BAK05B02) and the Natural Science Foundation Project of CQ CSTC (2012jjB30004 and 2012jjA30005).

References

Azzoni, A. and de Freitas, M.: Experimental gained parameters, decisive for rock fall analysis, Rock Mech. Rock Eng., 28, 111–124, 1995.

Bertolo, P., Oggeri, C., and Peila, D.: Full-scale testing of draped nets for rock fall protection, Can. Geotech. J., 46, 306–317, 2009.

Bhatti, A. Q. and Kishi, N.: Impact response of RC rock-shed girder with sand cushion under falling load, Nucl. Eng. Des., 240, 2626–2632, 2010.

Castro-Fresno, D., del Coz Diaz, J., López, L., and Nieto, P. G.: Evaluation of the resistant capacity of cable nets using the finite element method and experimental validation, Eng. Geol., 100, 1–10, 2008.

Cazzani, A., Mongiov, L., and Frenez, T.: Dynamic finite element analysis of interceptive devices for falling rocks, Int. J. Rock Mech. Min., 39, 303–321, 2002.

Chau, K. T., Wong, R. H., and Wu, J. J.: Coefficient of restitution and rotational motions of rockfall impacts, Int. J. Rock Mech. Min., 39, 69–77, 2002.

Delhomme, F., Mommessin, M., Mougin, J. P., and Perrotin, P.: Behavior of a structurally dissipating rock-shed: experimental analysis and study of punching effects, Int. J. Solids Struct., 42, 4204–4219, 2005.

Delhomme, F., Mommessin, M., Mougin, J. P., and Perrotin, P.: Simulation of a block impacting a reinforced concrete slab with a finite element model and a mass-spring system, Eng. Struct., 29, 2844–2852, 2007.

EOTA: ETAG 027 – Guideline for European Technical Approval of Falling Rock Protection Kits, Tech. rep., European Organization for Technical Approvals, Brussels, 2008.

Gerber, W.: Guideline for the Approval of Rockfall Protection Kits, Swiss Agency for the Environment, Forests and Landscape (SAEFL) and the Swiss Federal Research Institute WSL, Berne, 2001.

Giani, G., Giacomini, A., Migliazza, M., and Segalini, A.: Experimental and theoretical studies to improve rock fall analysis and protection work design, Rock Mech. Rock Eng., 37, 369–389, 2004.
Guzzetti, F., Crosta, G., Detti, R., and Agliardi, F.,: Stone: a computer program for the three-dimensional simulation of rock-falls, Comput. Geosci., 28, 1079–1093, 2002.
Kawahara, S. and Muro. T.: Effects of dry density and thickness of sandy soil on impact response due to rockfall, J. Terramechanics, 43, 329–340, 2006.
Kirsten, H.: Design and construction of Kowyon's pass rockfall shelter, J. S. Afr. Inst. Civ. Eng., 24, 477–492, 1982.
Kishi, N., Konno, H., Ikeda, K., and Matsuoka, K.: Prototype impact tests on ultimate impact resistance of PC rock-sheds, Int. J. Impact. Eng., 27, 969–985, 2002.
Labiouse, V., Descoeudres, F., and Montani, S.: Experiment study of rock sheds impacted by rock blocks, Structural Engineering International, 6, 171–176, 1996.
Mougin, J. P., Perrotin, P., Mommessin, M., Tonnelo, J., and Agbossou, A.: Rock fall impact on reinforced concrete slab: an experimental approach, Int. J. Impact. Eng., 31, 169–183, 2005.
Peila, D. and Ronco, C.: Technical Note: Design of rockfall net fences and the new ETAG 027 European guideline, Nat. Hazards Earth Syst. Sci., 9, 1291–1298, doi:10.5194/nhess-9-1291-2009, 2009.
Pichler, B., Hellmich, C. H., and Mang, H.: Impact of rocks onto gravel design and evaluation of experiments, Int. J. Impact. Eng., 31, 559–578, 2005.
Sasiharan, N., Muhunthan, B., Badger, T., Shu, S., and Carradine, D.: Numerical analysis of the performance of wire mesh and cable net rockfall protection systems, Eng. Geol., 88, 121–132, 2006.
Spadari, M., Giacomini, A., and Hambleton, J.: Prediction of the bullet effect for rockfall barriers: a scalling approach, Rock Mech. Rock Eng., 45, 131–144, 2012.
Topal, T., Akin, M., and Ozden, U.: Assessment of rockfall hazard around Afyon Castle, Turkey, Eng. Geol., 53, 191–200, 2007.
Volkwein, A., Schellenberg, K., Labiouse, V., Agliardi, F., Berger, F., Bourrier, F., Dorren, L. K. A., Gerber, W., and Jaboyedoff, M.: Rockfall characterisation and structural protection – a review, Nat. Hazards Earth Syst. Sci., 11, 2617–2651, doi:10.5194/nhess-11-2617-2011, 2011.

Table 1. The time elapse from the first contact of the block with the flexible rock-shed.

The key point frames of video camera	Time elapse (s)
Block contacting with rock-shed	0
Block down to the lowest point and steel vaulted structure beginning to rebound.	0.143
Block rebounding and steel vaulted structure stopping rebounding.	0.227
Block rebounding off flexible rock-shed	0.533
Block flying off one side of rock-shed	1.617

NHESSD
1, 4063–4086, 2013

Table 2. The maximum deformation of flexible nets and load on the cable anchor and horizontal cable.

Item	Maximum deformation of flexible nets (m)	Load on the cable anchor (kN)	Load on the horizontal cable (kN)
Results	2.310	21.4	29.5

NHESSD
1, 4063–4086, 2013

Fig. 1. Rock-shed with reinforced concrete columns, foundation and a roof slab.

NHESSD
1, 4063–4086, 2013

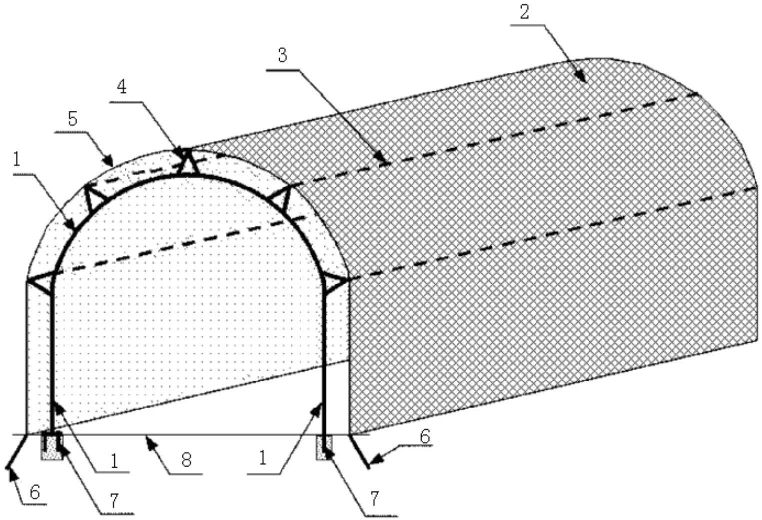

Fig. 2. Flexible rock shed composed of steel vaulted structure and flexible nets. 1. Steel vaulted structure; 2. flexible nets; 3. longitudinal support cables; 4. net-hanging bracket; 5. hoop support cable; 6. cable anchors; 7. anchor bolt; 8. ground.

NHESSD
1, 4063–4086, 2013

Flexible rock-shed under the impact of rock block

S. Shi et al.

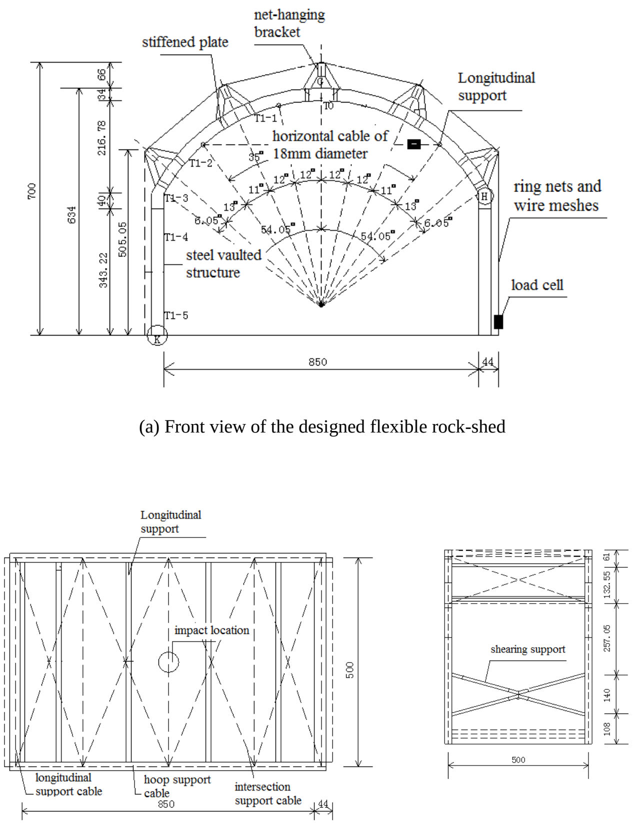

(a) Front view of the designed flexible rock-shed

(b) Top view of the flexible rock-shed

(c) End view of the flexible rock-shed

Fig. 3. The design of a single-span flexible rock-shed.

NHESSD
1, 4063–4086, 2013

Title Page
Abstract | Introduction
Conclusions | References
Tables | Figures
◀I | ▶I
◀ | ▶
Back | Close
Full Screen / Esc
Printer-friendly Version
Interactive Discussion

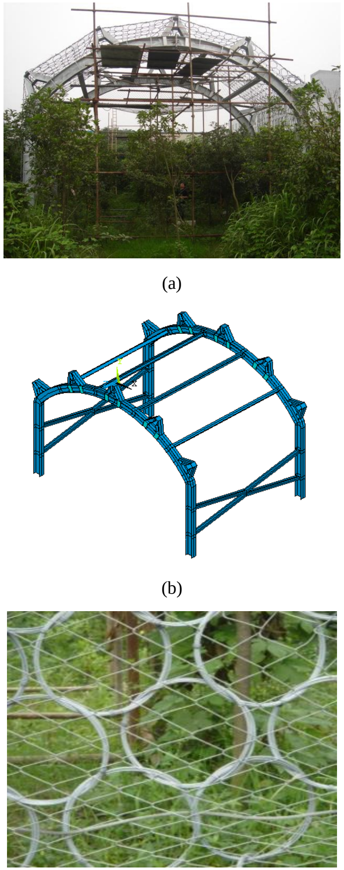

(a) (b) (c)

Fig. 4. (a) Flexible rock-shed; **(b)** steel vaulted structure; **(c)** ring nets with diameter 300 mm and TECCO wire meshes G65.

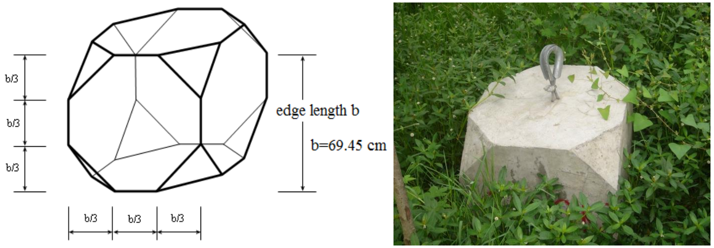

(a)

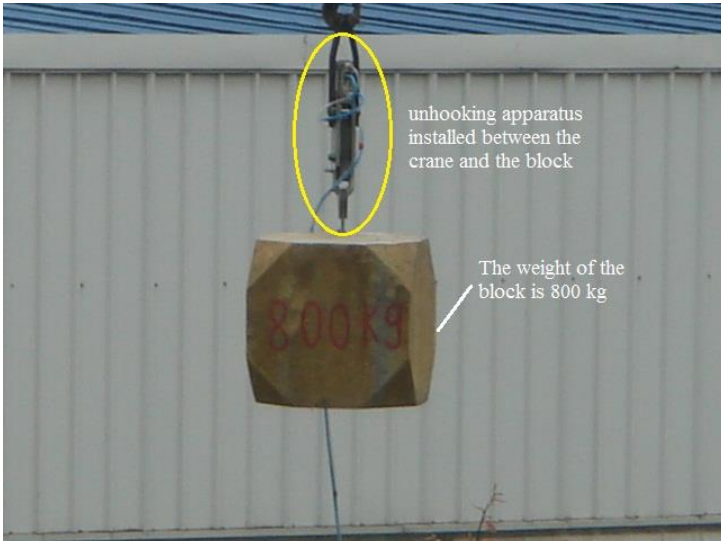

(b)

Fig. 5. (a) Cubic block of 14-face polyhedron; **(b)** an unhooking apparatus installed between the crane and the block.

NHESSD
1, 4063–4086, 2013

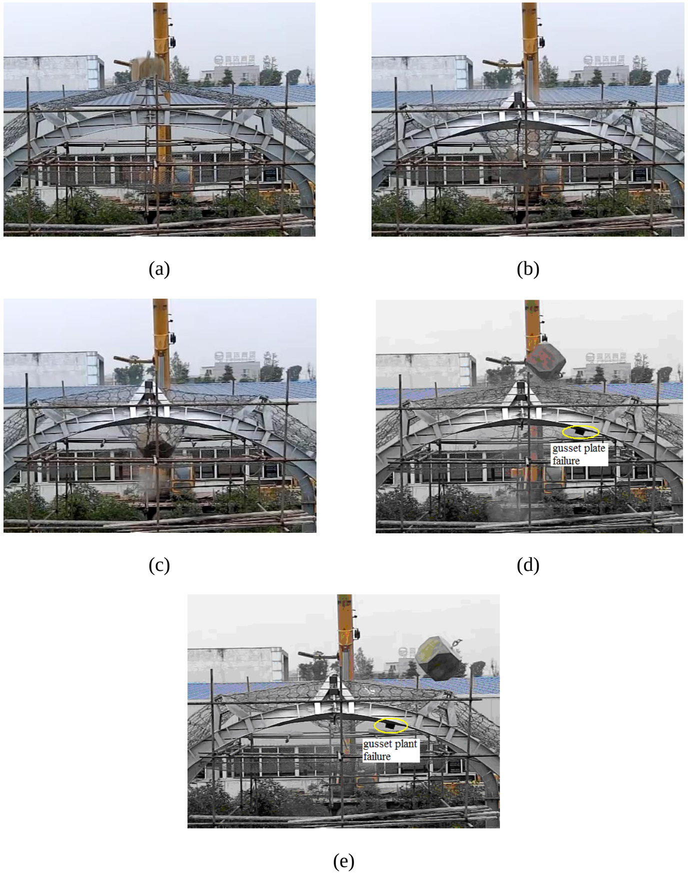

Fig. 6. Key point frames of video camera. **(a)** Block contacting with rock-shed; **(b)** block down to the lowest point and steel vaulted structure beginning to rebound; **(c)** block still rebounding and steel vaulted structure stopping rebounding; **(d)** block rebounding off flexible rock-shed; **(e)** block flying off one side of rock-shed.

NHESSD
1, 4063–4086, 2013

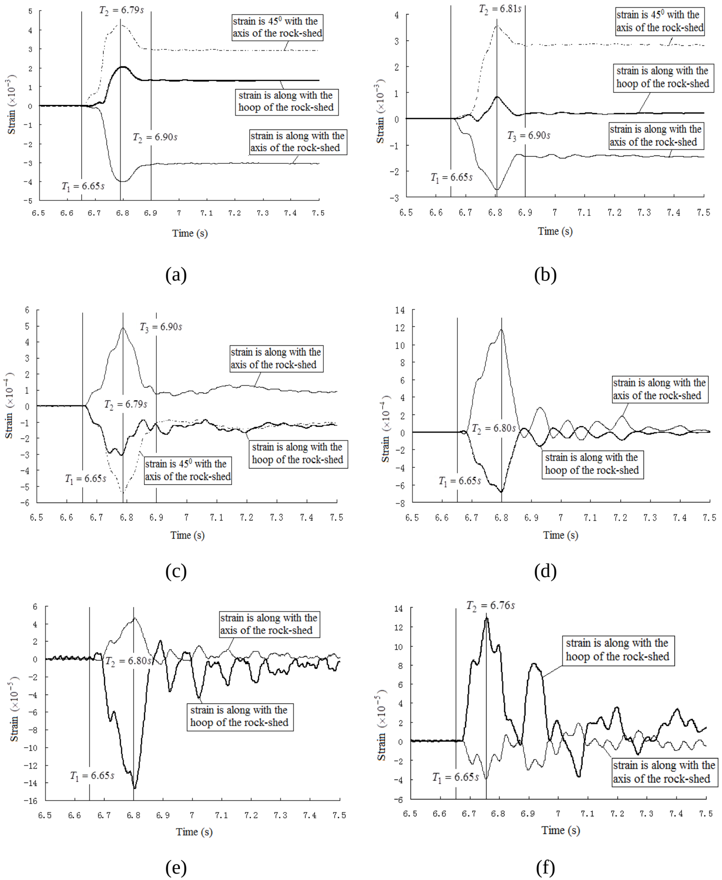

Fig. 7. The time-strain diagrams as recorded by the strain gauges. **(a)** Time-strain diagram at T0; **(b)** time-strain diagram at T1-1; **(c)** time-strain diagram at T1-2; **(d)** time-strain diagram at T1-3; **(e)** time-strain diagram at T1-4; **(f)** Time-strain diagram at T1-5.

(a)

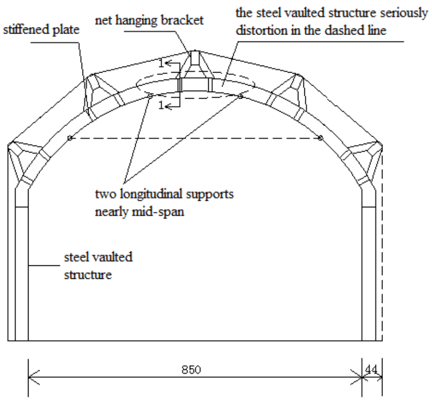

(b)

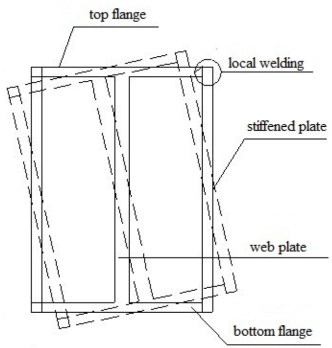

(c)

Fig. 8. The most serious distortion occurred between the two longitudinal supports nearly mid-span. **(a)** The picture of the distorted arched beam; **(b)** the schematic distortion drawing of the structure; **(c)** the detail cross sectional deformation of arch beams.

NHESSD
1, 4063–4086, 2013

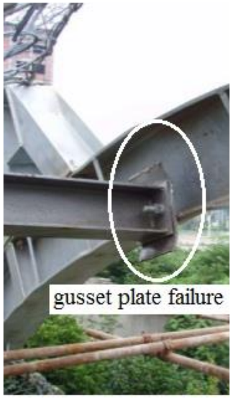

(a)

(b)

Fig. 9. (a) One of the gusset plates failure; **(b)** the detail deformation at the gusset plates.

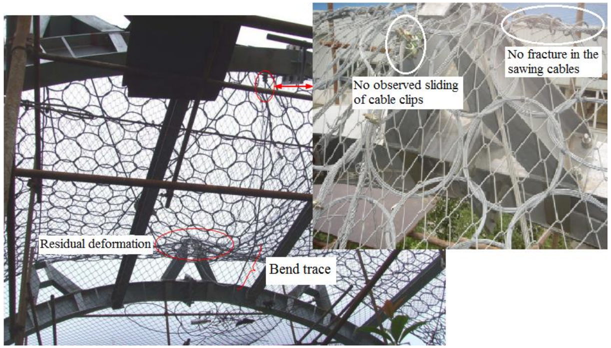

(a)

(b)

Fig. 10. The detail deformation of the components in the flexible rock-shed after the impact of the rock block.

NHESSD
1, 4063–4086, 2013

Title Page
Abstract | Introduction
Conclusions | References
Tables | Figures
◀| |▶
◀ ▶
Back | Close
Full Screen / Esc
Printer-friendly Version
Interactive Discussion